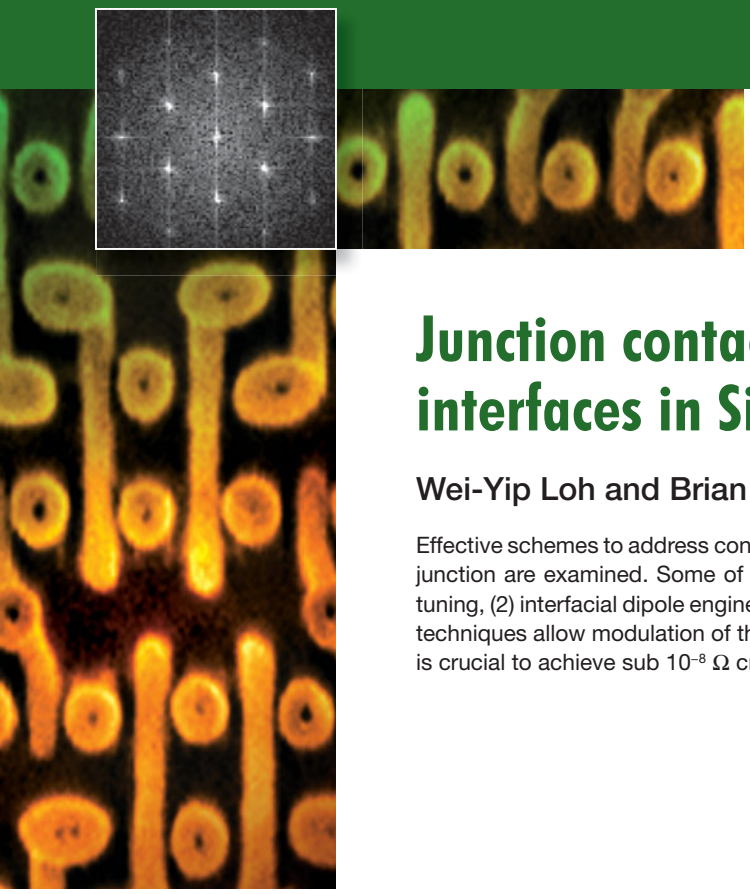


Junction contact materials and interfaces in Si channel devices

Wei-Yip Loh and Brian Coss

Effective schemes to address contact resistance between silicide and a highly doped diffused junction are examined. Some of the techniques introduced include (1) metal work function tuning, (2) interfacial dipole engineering, and (3) phase modulation of the nickel silicide. These techniques allow modulation of the Schottky barrier of NiSi to *n*-Si to less than 0.3 eV, which is crucial to achieve sub 10^{-8} Ω cm^2 contact resistivity for the sub-32 nm technology node.

Introduction

Semiconductor to metal contact engineering and contact material development have become crucial in recent years to keep pace with the continual improvement in electronic device performance. As device dimensions shrink and device performance improves, increasing current densities in devices is causing the semiconductor-metal contacts and semiconductor junctions to severely affect the device performance. This will require new contact materials and innovative materials engineering to cater to complementary metal-oxide semiconductors (CMOS) in dual *n*-type and *p*-type contacts requirements. In addition, introduction of new device architectures such as FinFET (fin-shaped field-effect transistor) and nanowire FETs is also accompanied by technological challenges in contacts, such as requirements for three-dimensional contact schemes.

This review focuses on some of the key issues in the development of contact materials for advanced Si CMOS technologies. Various ways to engineer highly conductive silicide contacts (see **Figure 1** in the article by Wen and Chambers in this issue) for a sub-32 nm technology node will be explored. Techniques of lowering Schottky barrier height (SBH) in nickel silicide by usage of low work function metals, improved carrier concentration via dopant segregation, implanted impurity, and silicide phase modulation will be discussed, with particular focus on the technology requirement of contact pitch scaling for a sub-32 nm technology node.

Silicide contacts

Ohmic contacts to semiconductors have typically been achieved through a single metal or silicide to degenerately doped silicon. For sub-50 nm gate length, the contribution of the contact resistance R_{co} (or contact resistivity ρ_{CO} when normalized by area), which is the resistive component from the metal silicide to the highly doped source drain, is expected to dominate over other parasitic components.[1] Yu proposed a theoretical model for thermionic field emission between the metal/silicide and silicon, which shows ρ_{CO} is directly proportional to the SBH, ϕ_B, and is inversely proportional to the square root of the dopant concentration, N_d, in the semiconductor.[2] See Equation 1 in the introductory article of this issue.

Work function modulation

While NiSi has a low Schottky barrier to *p*-Si(100), ϕ_{Bp}, it has a complementary high Schottky barrier, ϕ_{Bn}, of 0.65–0.7 eV on *n*-Si(100), since $\phi_{Bn} + \phi_{Bp} = 1.1$ eV (Si bandgap). Using rare-earth metals (which have one of the lowest metal work functions), Tu et al. have shown a low ϕ_{Bn} of 0.37–0.39 eV for disilicides of Dy, Er, Gd, Ho, and Y to *n*-Si.[3] Further studies also have shown that a very high hole Schottky barrier ϕ_{Bp} of 0.82 eV

Wei-Yip Loh, Sematech, Austin, TX, USA; wei-yip.loh@sematech.org
Brian Coss, Sematech, Austin, TX, USA; brian.coss@student.utdallas.edu
DOI: 10.1557/mrs.2011.7

© 2011 Materials Research Society

https://doi.org/10.1557/mrs.2011.7 Published online by Cambridge University Press

(corresponding to ϕ_{Bn} ~0.27 eV assuming $\phi_{Bn} = E_g - \phi_{Bp}$) can be obtained with $YbSi_2$.[4] Instead of adopting the dual silicide (for *n*- and *p*-type contact) approach, an alternative is to use a single silicide but to incorporate the rare-earth impurities into the NiSi/Si interface. **Figure 1a** shows the measured ϕ_{Bn} of nickel silicide with different metal implanted into *n*-Si prior to the nickel silicidation (the "pre-silicide" state). The rare-earth metal is implanted into the *n*-Si prior to the nickel deposition at a similar dose of $1 \times 10^{13}/cm^2$ but with a slightly different energy to achieve the same projected range (to cater to the difference in rare-earth metal atomic mass). Secondary ion mass spectroscopy depth profile of the subsequent nickel silicide shows segregation of the rare-earth at the NiSi/Si interface, which is similar in behavior to dopant segregation in nickel silicide.[8,9]

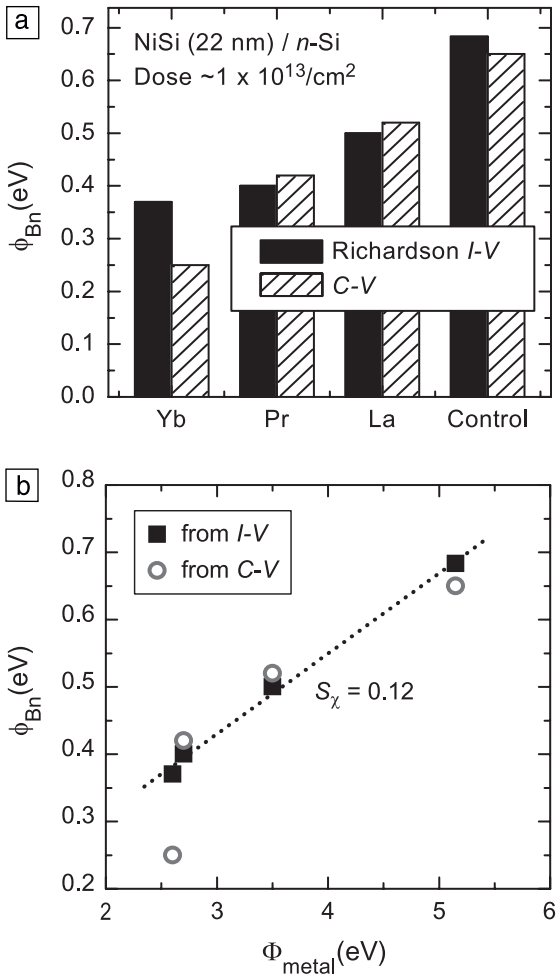


Figure 1. (a) Schottky barrier height (SBH) of NiSi on *n*-Si with various pre-silicide implants (implant fluence of $1 \times 10^{13}/cm^2$). SBH, ϕ_{Bn} is measured using a Richardson plot of reverse leakage current[6] at 0.5 V and depletion capacitance-voltage (*C-V*) measurements[6,7] at 100 kHz. A significant discrepancy is observed in the ϕ_{Bn} measurement from Richardson plot and depletion *C-V* for Yb, and this is attributed to frequency-dependent traps response during the *C-V* measurement. Reprinted with permission from Reference 5. © 2010, American Institute of Physics, (b) Measured SBH for NiSi on *n*-Si with various pre-silicide metal impurities versus the metal work function. A less than unity interface index S_χ, as defined in Equation 2, shows an imperfect interface with a high degree of Fermi-level pinning.

According to Mott-Schottky theory,[10,11] the SBH, ϕ_B, between a metal/silicide with a work function of Φ_M and a semiconductor with electron affinity χ is given by

$$\phi_B = \Phi_M - \chi. \quad (1)$$

Equation 1 suggests a unity slope between ϕ_B and metal/silicide work function Φ_M, with $\partial\varphi_B / \partial\Phi_M = 1$. In reality, most experimental results show various degrees of Fermi-level pinning, with a less than unity interface index S_χ defined as

$$S_\chi = \partial\phi_B / \partial\Phi_M < 1. \quad (2)$$

Low values of S_χ are observed, especially in covalent semiconductors (e.g., Si and Ge). Figure 1b shows the correlation between the measured ϕ_{Bn} and the work function of the rare-earth metal and control samples with Ni. A linear correlation between the measured ϕ_{Bn} and metal work function is observed, although the slope $S_\chi = 0.12$ is much lower than unity. This agrees with the Fermi-level pinning effects observed in the studies by Tung[12] and Kurtin,[13] which show a low S_χ of between 0.1 to 0.2 for silicon. The effective modulation of ϕ_B in implanted rare-earth impurities NiSi shows that pre-silicide ion-implantation can be a viable alternative to dual metal silicides.

Interfacial dielectric dipole engineering

The low interface index S_χ for Si suggests that interface properties rather than bulk properties such as metal work function govern the actual ϕ_B. Two main theories explaining the mechanism have been proposed: (1) Dipole formation due to bond polarization at the metal-semiconductor interface and (2) metal-induced gap states (MIGS), which explain Fermi-level pinning in a metal-semiconductor coupling as the extension of the metal wave function into the semiconductor. The MIGS theory assumes that the metal/silicide induces the gap states, but the actual density of the gap states is dependent on the semiconductor.[14,15] According to the MIGS theory, passivating the gap states of the underlying semiconductor will relieve the Fermi-level pinning effect, and hence recover the unity relation between ϕ_B and the metal work function.

Several groups have reported great success in relieving the Fermi-level pinning effect by the insertion of an ultrathin dielectric into various semiconductors. Connelly et al. showed Mg and Yb contacts to *n*-Si with interfacial silicon nitride that demonstrate a low barrier height of 0.2 eV.[16] Similiarly, Takahashi et al.[17] and Kobayashi et al.[18] both separately demonstrated good device performance on a Ge substrate using metal-to-Ge with an interfacial GeO_x or SiN layer, respectively. An alternative approach is to use an interfacial layer that both passivates and incorporates dipoles to help modulate the final ϕ_B.[19,20] **Figure 2** shows the near band-edge SBH using TaN with AlO_x/SiO_2 or LaO_x/SiO_2 interfacial dipoles. The LaO_x and AlO_x dielectrics are deposited onto a clean *n*-Si, and interfacial SiO_2 is formed

https://doi.org/10.1557/mrs.2011.7 Published online by Cambridge University Press

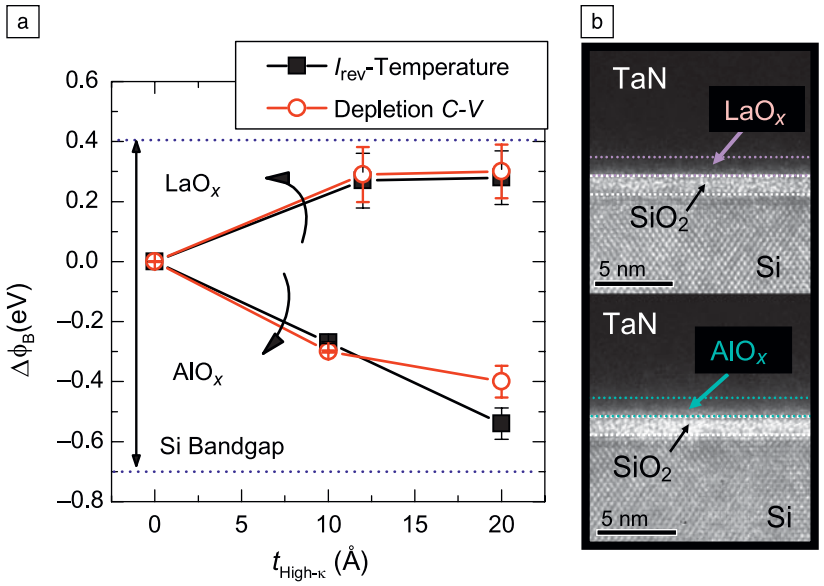


Figure 2. (a) Schottky barrier height (SBH [ϕ_B]) tuning as a function of AlO$_x$ and LaO$_x$, high-κ thickness on *p*-Si calculated with respect to TaN/*p*-Si control. Nearly band-edge SBHs are obtained using LaO$_x$ and AlO$_x$ on *p*-Si. (b) A transmission electron microscopy image of 10 nm of LaO$_x$ and AlO$_x$ capped with TaN metal on a *n*+Si substrate. Reprinted with permission from Reference 20. © 2009, American Institute of Physics.

naturally during the annealing cycle due to the difference in electronegativity and oxygen affinity. The inclusion of about 1 nm of high-κ dielectrics is able to both passivate and modulate the ϕ_{Bn} of TaN on *n*-Si by more than 0.2 eV, achieving close to band edge modulation with 2 nm of dielectrics. The observed ϕ_B shifts correspond closely to the reported dipole moment for AlO$_x$/SiO$_2$ and LaO$_x$/SiO$_2$ interfaces.[21] While higher dielectric thickness incorporates higher amounts of dipoles, tunneling probability is also reduced due to the enhanced thickness, and hence optimization of the process is required for contact application. Due to the conformal deposition of high-κ dielectrics or SiN, this contact scheme can ideally be implemented in any two- or three-dimensional contact structure.

Phase modulation of nickel silicides

Nickel is known to form three different phases of silicide (Ni$_2$Si, NiSi, and NiSi$_2$), depending on the annealing temperature.[22,23] At temperatures <350°C, Ni-rich Ni$_2$Si is formed with intermediate resistivity and high ϕ_{Bn}, while at temperatures >750°C, a Si-rich NiSi$_2$ phase is formed with ϕ_{Bn} ranging from 0.4 eV to 0.65 eV,[23,24] but with significantly higher resistivity. Using nitrogen implantation, a phase-modulated Ni silicide has been demonstrated for CMOS integration at the same silicidation temperature.[25] **Figure 3** shows the cross-sectional transmission electron microscopy images of the control NiSi (unimplanted sample) and samples on Si(100) with a high dose (3.5×10^{15}/cm^2) of N implanted before Ni deposition. The resistivity of the N-implanted NiSi is higher than NiSi but significantly lower than NiSi$_2$. In addition, implanted samples also show pyramidal silicide at the {111} facet, which is attributable to preferential NiSi$_2$ formation along the Si(111) plane, although these facets are sparse.

The electrical characteristics of N-implanted NiSi also have been studied. **Figure 4a** shows the Schottky barrier extracted from a Richardson plot using the reverse leakage for both control NiSi (without pre-silicide implant) and N-pre-silicide implanted samples, with temperatures ranging from 300 K to 400 K. For the N-implanted dose of $> 1 \times 10^{15}$/cm^2, the Schottky barrier, ϕ_{Bn}, reduces from the control of 0.7 eV to about 0.34 eV. The large reduction in ϕ_{Bn} is consistent with reported Schottky barriers for NiSi$_2$.[26] A source/drain dopant segregated *n*-channel MOSFET with N-pre-silicide implanted NiSi has been fabricated and characterized.[25] Figure 4b shows the extracted total resistance from drive current at overdrive of gate voltage, $V_g - V_t = 1.0$ V (where V_t is the threshold voltage) as a function of different gate length, L_g. Series resistance R_{ext} for N-implanted samples shows a 22% reduction, due mainly to R_{co} reduction.

Summary for silicide contacts

This article discusses the various schemes for modulating the Schottky barrier height ϕ_B to reduce contact resistivity. Significant progress in tuning the ϕ_B has been achieved using low work function metals such as YbSi$_2$ ($\phi_{Bn} < 0.3$ eV)[4] or by pre-silicide ion-implantation and segregation ($\phi_{Bn} < 0.4$ eV). To relieve the Fermi-level pinning observed mainly in Si and Ge with covalent bonds, interfacial layer engineering has reduced

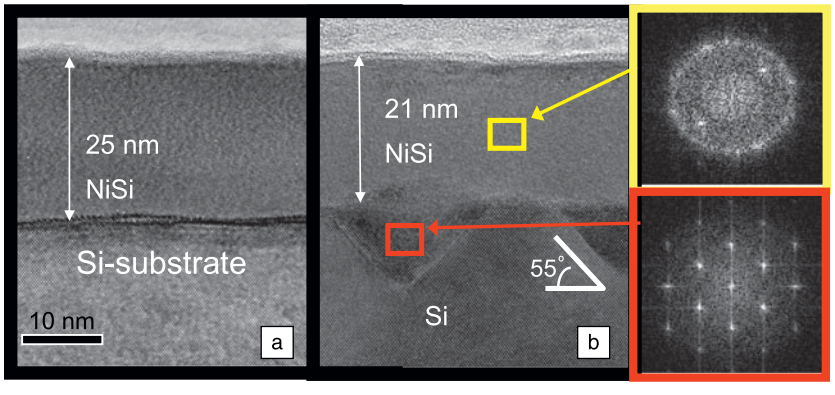


Figure 3. High-resolution transmission electron microscopy micrograph of (a) control NiSi without a N-implant and (b) with a N-implant (3.5×10^{15} N/cm^2). NiSi with a N-implant shows a thinner silicide with facets observed at the Si(111) interface. The scale is the same for (a) and (b). Fast Fourier transforms (FFTs) (right) on bulk Ni silicide and on the interfacial facets for samples with N-implant are also shown. FFTs on interfacial facets show fcc structures, epitaxial to the underlying Si substrate.

https://doi.org/10.1557/mrs.2011.7 Published online by Cambridge University Press

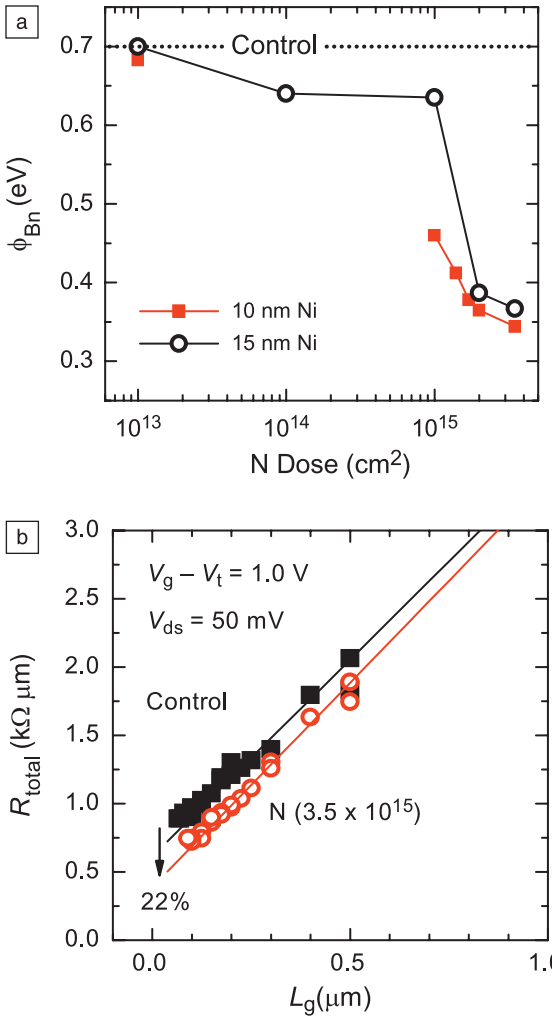


Figure 4. (a) Summary of electron ϕ_{Bn} for various doses of N-implant. At high dose, N-implanted samples show ϕ_{Bn} close to typical values for $NiSi_2$. Solid symbols reflect data for thin 10 nm Ni, while open symbols show data for thicker Ni silicide with 15 nm of deposited Ni. (b) Total device resistance (R_{total}) as a function of printed gate length, L_g, in dopant-segregated source/drain (DSS) *n*-channel MOSFETs. Control samples without nitrogen implant are shown as solid symbols, while open symbols reflect data for N-implanted samples. N-implanted DSS-nFETs show a 22% reduction in R_{total} compared to control due to a reduction in R_{co}.

ϕ_{Bn} of metal-to-*n*-Si to 0.2 eV.[16] Complementary metal oxide semiconductor compatible dielectric dipole mitigated contacts have also been demonstrated, which could reduce ϕ_B to both *n*-Si and *p*-Si by insertion of LaO_x or AlO_x, respectively.[19,20] Finally, phase modulation of NiSi is observed when nitrogen is implanted prior to silicidation. Nitrogen acts as a Ni diffusion barrier and enhances $NiSi_2$ interfacial formation, which reduces ϕ_{Bn} from nominal values of 0.7 eV to 0.34eV.[25] The various schemes show substantial ϕ_{Bn} modulation down to 0.3 eV, which is critical for achieving sub 10^{-8} Ωcm^2 contact resistivity for the sub-32 nm technology node.

References

1. S.-D. Kim, C.-M. Park, C.S. Woo, *IEEE Trans. Electron Dev.* **49** (3), 467 (2002).
2. A.Y.C. Yu, *Solid-State Electron.* **13**, 239 (1970).
3. K.N. Tu, R.D. Thompson, B.Y. Tsaur, *Appl. Phys. Lett.* **38** (8), 626 (1981).
4. S. Zhu, J. Chen, M.-F. Li, S.J. Lee, J. Singh, C.X. Zhu, A. Du, C.H. Tung, A. Chin, D.L. Kwong, *IEEE Electron Dev. Lett.* **25** (8), 565 (2004).
5. W.-Y. Loh, S. Felch, H. Etienne, I. Ok, D. Turnbaugh, Y. Spiegel, F. Torregrosa, L. Roux, P. Majhi, R. Jammy, *18th Int. Conf. on Ion Implantation Tech.* 1321 (2010).
6. K. Chino, *Solid-State Electron.* **16**, 119 (1973).
7. S.M. Sze, *Physics of Semiconductor Devices, 2nd Edition* (Wiley, New York, 1981).
8. A. Kinoshita, C. Tanaka, K. Uchida, J. Koga, *Symp. VLSI Technol.* **158**, (2005).
9. M. Zhang, J. Knoch, Q.T. Zhao, U. Breuer, S. Mantl, *Solid-State Electronics* **50**, 594 (2006).
10. W. Schottky, *Z. Phys.* **113**, 367 (1939).
11. N.F. Mott, *Proc. R. Soc.* **171**, 27 (1939).
12. R.T. Tung, *J. Vac. Sci. Technol., B* **11**, 1546 (1993).
13. S. Kurtin, T.C. McGill, C.A. Mead, *Phys. Rev. Lett.* **22**, 1433 (1970).
14. C. Tejedor, F. Flores, E. Louis, *J. Phys. C: Solid State Phys.* **10**, 2163 (1977).
15. R.T. Tung, *Mater. Sci. Eng., R* **35**, I–138 (2001).
16. D. Connelly, C. Faulkner, D.E. Grupp, J.S. Harris, *IEEE Trans. Nanotechnology* **3**, 1 (2004).
17. T. Takahashi, T. Nishimura, L. Chen, S. Sakata, K. Kita, A. Toriumi, *Int. Electron Dev. Meet. Tech Dig.* **697** (2007).
18. M. Kobayashi, A. Kinoshita, K. Saraswat, H.-S.P. Wong, Y. Nishi, *Symp. VLSI Technol.* **54** (2008).
19. B.E. Coss, W.-Y. Loh, J. Oh, G. Smith, C. Smith, H. Adhikari, B. Sassman, S. Parthasarathy, J. Barnett, P. Majhi, R.M. Wallace, J. Kim, R. Jammy, *Symp. VLSI Technol.* **104** (2009).
20. B. Coss, W.-Y. Loh, R.M. Wallace, J. Kim, P. Majhi, R. Jammy, *Appl. Phys. Lett.* **95**, 222105 (2009).
21. K. Kita, A. Toriumi, *IEDM Tech Dig.* **29**(2008).
22. A. Lauwers, A. Steegen, M. de Potter, R. Lindsay, A. Satta, H. Bender, K. Maex, *J. Vac. Sci. Technol., B* **19** (6), 2026 (2001).
23. F. d'Heurle, C.S. Peterson, J.E.E. Baglin, S.J. La Placa, C.Y. Wong, *J. Appl. Phys.* **55** (12), 4208 (1984).
24. H. Fujitani, *Phys. Rev. B* **50** (12), 8681(1994).
25. W.-Y. Loh, P.Y. Hung, B.E. Coss, P. Kalra, I. Ok, G. Smith, C.-Y. Kang, S.-H. Lee, J. Oh, B. Sassman, P. Majhi, P. Kirsch, H.-H. Tseng, R. Jammy, *Symp. VLSI Technol.* **100** (2009).
26. R.T. Tung, A.F.J. Levi, J.P. Sullivan, F. Schrey, *Phys. Rev. Lett.* **66** (1), 72 (1991). □

Need to Connect with the Materials Research Society?

Click www.mrs.org

Call 724.779.3003

Fax 724.779.8313

Write info@mrs.org

https://doi.org/10.1557/mrs.2011.7 Published online by Cambridge University Press